*Macedonian Journal of Chemistry and Chemical Engineering*, Vol. **45**, No. 1, pp. xx–xx (2026)

MJCCA9 –

ISSN 1857-5552
e-ISSN 1857-5625

Received: January 25, 2026
Accepted: February 10, 2026

DOI: 10.20450/mjcce.2026.3433
*Original scientific paper*

# DECODING THE FEATURES OF BIOCHEMICAL MULTISTEP ELECTRON-TRANSFER PATHWAYS WITH THE TWO-STEP DOUBLE-REGENERATIVE ELECTROCHEMICAL MECHANISM IN SQUARE-WAVE VOLTAMMETRY

**Rubin Gulaboski**

*Faculty of Medical Sciences, Goce Delčev University, Štip, North Macedonia*

rubin.gulaboski@ugd.edu.mk

Results from theoretical analyses of a two-step double-regenerative electrochemical mechanism (schematically expressed as the EC′EC″ mechanism) are presented here and examined for the first time under conditions of square-wave voltammetry. The primary emphasis is on the relevance of this complex mechanism in terms of gaining a more comprehensive understanding of analogous mechanistic pathways that frequently operate under physiological conditions. Such complex mechanistic schemes are typical of many biologically important pathways in which coupled electron-transfer steps are linked to homogeneous regenerative reactions mediated by catalytic substrates, enzymes, stable radical species, or certain redox cofactors. Through systematic analysis of the forward and backward square-wave current components, we elucidate the role of the regenerative loops associated with both electron-transfer steps in affecting the voltammetric response and generating distinct electrochemical–catalytic signatures. The proposed framework is the first to encompass the interplay between electron-transfer kinetics, chemical regeneration rates, and mass transport within the time scale imposed by a square-wave excitation signal. The results establish a useful framework for a unified mechanistic interpretation of complex bioelectrochemical systems, while offering a robust theoretical basis for kinetic analyses of multistep redox pathways relevant to metabolic processes, enzymatic catalysis, and redox signaling in living organisms.

**Keywords**: EC′ catalytic reaction mechanism; enzyme-substrate kinetics; multistep redox mechanisms; electrochemical-catalytic loops; EC′EC″ electrochemical mechanism.

## ДЕКОДИРАЊЕ НА КАРАКТЕРИСТИКИТЕ НА БИОХЕМИСКИТЕ ПОВЕЌЕСТЕПЕНИ ЕЛЕКТРОДНИ МЕХАНИЗМИ ПРЕКУ СВОЈСТВАТА НА ДВОСТЕПЕН ДВОЈНО РЕГЕНЕРАТИВЕН ЕЛЕКТРОХЕМИСКИ МЕХАНИЗАМ ВО УСЛОВИ НА КВАДРАТНО-БРАНОВА ВОЛТАМЕТРИЈА

Резултатите од теоретските анализи на двостепен двојнорегенеративен електрохемиски механизам (дефиниран како ЕС′ЕС″) за првпат се презентирани во рамките на овој труд, при што се направени анализи во услови на квадратнобрановата волтаметрија. Главниот акцент во трудот е ставен на релевантноста на овој комплексен електрохемиски механизам во насока на подобро разбирање на аналогни механистички патеки што често се одвиваат кај голем број биохемиски системи при физиолошки услови. Ваквите комплексни механистички шеми се карактеристични за важни биолошки процеси, каде што процесите на пренос на електрони најчесто се поврзани со регенеративни хемиски реакции, со посредство на каталитички супстрати, ензими, стабилни радикали или одредени редокс-кофактори.

Преку систематска анализа на директните и повратните волтамограми на струјните квадратно-бранови компоненти се направени обиди да се објасни улогата на регенеративните процеси поврзани со двата чекора на електронски трансфер, како во обликувањето на волтаметриски одговор така и во генерирањето на карактеристични електрохемиско-каталитички

отпечатоци за овој сложен механизам. Предложениот алгоритам за првпат ја разгледува меѓусебната интеракција помеѓу кинетиката на преносот на електрони, процесите на хемиската регенерација и транспортот на масата во текот на временската скала дефинирана преку квадратно-брановата фреквенција. Добиените резултати од овие анализи претставуваат корисна основа за унифицирана механистичка интерпретација на комплексни биоелектрохемиски системи. Покрај тоа, резултатите од овој труд претставуваат стабилна теоретска подлога за кинетичка анализа на повеќестепени редокс-механизми релевантни за метаболичките процеси, за процесите на ензимска катализа, како и за објаснување на редокс-сигнализацијата во живите организми.

**Клучни зборови:** EC′ каталитички електроден механизам; кинетика на ензимско-супстратни реакции; повеќестепени електрохемиски механизми; електрохемиски-каталитички отпечатоци; EC′EC″ електрохемиски механизам

## 1. INTRODUCTION

Electrochemical mechanisms that involve a regenerative chemical reaction following an electron-transfer step, commonly referred to in electrochemistry as EC′ mechanisms,[1–7] play a fundamental role in the interpretation of the redox processes that occur in important chemical and biological systems.[1,5] The electrochemical concept of the EC′ mechanistic pathway is based on the idea that the product of the electron transfer undergoes a subsequent irreversible homogeneous reaction with a chemical species present in solution, while regenerating the initial electroactive reactant.[1,3–7] This type of electrochemical-catalytic (or regenerative) loop produces a specific current amplification and distinct voltammetric signatures, making EC′ reaction mechanisms easily recognizable under voltammetric conditions.[1–7] The EC′ mechanistic pathways are of the utmost importance for the study of enzymatic catalysis, redox mediation in various multistep electrode transformations, and bioelectrochemical sensing.[1,2,5,6] Extensive theoretical studies of various aspects of the EC′ mechanism under voltammetric conditions have been conducted, and valuable contributions related to this mechanism can be found in.[1–8] Most of the theoretical studies of EC′ mechanisms have aimed to elucidate how the chemical kinetics shapes voltammetric responses, and how voltammetric techniques can be employed to evaluate the kinetic parameters relevant to a wide range of biochemical and physiological systems.

In many physiological systems, important redox molecules undergo not one but two consecutive electron-transfer steps, while forming stable intermediate species with different oxidation states.[9–16] Each of the redox products formed in this sequence may subsequently participate in a distinct regenerative reaction with a specific chemical substrate, thereby giving rise to a double-regenerative electrochemical pathway, referred to in this work as the EC′EC″ mechanism. Many biochemical systems naturally exhibit behavior that is consistent with the scheme represented by double-regenerative EC′EC″ mechanisms. Important redox cycles that include the electron transformation of quinone and semiquinone,[14–19] such as those involving ubiquinone (coenzyme Q10)[16–20] in mitochondrial electron transport, commonly undergo two sequential one-electron transformations. In a multi-step redox transformation of coenzyme Q10, both the intermediates (semiquinone radicals) and final products react rapidly with molecular oxygen under physiological conditions, while regenerating the parent compounds and producing a dual catalytic effect.[14–18] Flavin cofactors ($FAD/FADH_2$)[14–16] are chemical systems that are central to flavoproteins and oxidative enzymes, and form both stable intermediate radical species and fully reduced species that participate in separate regenerative reactions with oxygen, hydrogen peroxide, or other reactive oxygen species. Ascorbic acid (vitamin C) is oxidized through two one-electron steps, in which both oxidized forms (i.e., semidehydroascorbate radicals and dehydroascorbates) engage in irreversible reactions with other radicals or metal ions, while creating two catalytic feedback cycles.[20] In $NADH/NAD^+$-mediated biochemical systems, electrochemical oxidation often proceeds through radical intermediates that are enzymatically regenerated, resulting in multi-level catalytic behavior analogous to the EC′EC″ mechanism.[5,14–16,20] Similar double-regenerative electrochemical patterns appear in environmental redox molecules, such as various aromatic systems containing quinone moieties, phenols, arylamines, imines and many more.[16–20] These important examples demonstrate that EC′EC″ mechanisms are not only theoretically significant,[1–6,20–23] but also highly relevant in terms of describing the redox behavior of biologically and environmentally important molecules.

In the theoretical framework of the EC′EC″ mechanism considered in this work, both electron-transfer steps are coupled to irreversible chemical reactions that regenerate earlier redox forms, while producing two electrochemical–catalytic loops. Although "simple" single-step EC′ systems have been extensively analyzed,[1-8] the double-regenerative EC′EC″ mechanism has not yet been theoretically resolved under the kinetic regime of electron transfer steps under square-wave voltammetry (SWV) conditions. Unlike previously treated EEC′ or sequential EE systems coupled to a single catalytic loop, the EC′EC″ framework considered here explicitly incorporates two independent regenerative cycles, each of which feeds a different oxidation level. In view of the sensitivity of SWV to kinetic systems,[6] a theoretical framework for the EC′EC″ mechanism is necessary in order to understand the various coupled multi-step electrochemical reactions in biological and environmental pathways. Finally, it is important to emphasize that the algorithm used for the EC′EC″ mechanism considered here is different from both the well-established one-step catalytic EC′ mechanism[1–6] and from the EEC′ mechanism.[23] Moreover, this mechanism is distinct from multistep models that have been primarily developed for systems involving thermodynamically reversible electron-transfer steps.[13]

## 2. THEORETICAL FRAMEWORK

### 2.1. *Short explanation of the EC′EC″ reaction mechanism*

The EC′EC″ mechanism involves a two-step consecutive electrochemical transformation, in which the product of each electron-transfer step enters into an irreversible homogeneous chemical reaction that regenerates the previous reactant. The electrochemical process begins with a one-electron oxidation of an initial redox active species R (where R is the only electroactive reactant present in the electrochemical cell at the beginning of the experiment), which creates a stable intermediate species Ox1 via a one-electron transfer step at the electrode/electrolyte interface. Immediately after its formation, the Ox1 species can undergo an irreversible chemical reaction with a reagent Y (assumed to be present in excess in the voltammetric cell), while regenerating the initial reactant (i.e., species R) through a first catalytic pathway characterized by the rate constant $k_{c,1}$ (the EC′ step). In parallel, in the second electrochemical step, Ox1 can be further oxidized by a second one-electron transfer, forming the final product, i.e., the species Ox2 (for simplicity, the charges of all species are omitted). This newly generated species Ox2 also participates in an irreversible homogeneous reaction with the same reagent Y, while regenerating the intermediate redox active species Ox1. This second regenerative pathway (governed by rate constant $k_{c,2}$) constitutes the second or EC″ step of the entire mechanistic scheme. Together, these coupled electrode and chemical processes create a double electrochemical–regenerative cycle, where there is continuous feedback to each electrochemical sequence, as described in sequences (a)–(d) of (I).

**R - 1e-** ⇄ **Ox1** (first electron transfer step; ($k_{s,1;}\alpha_1$)) (a)

**Ox1** + **Y** → **R** + **S1** (C′ first regeneration reaction, $k_{c,1}$) (b)

**Ox1 - 1e-** ⇄ **Ox2** (second electron transfer step; ($k_{s,2;}\alpha_2$)) (c)

**Ox2** + **Y** → **Ox1** + **S2** (C″ second regeneration reaction, $k_{c,2}$) (d)

**Scheme I.** Reaction scheme showing the sequences (a–d) of the EC′EC″ mechanism, comprising two consecutive electron-transfer steps coupled with two homogeneous regenerative chemical reactions. The first and second electron-transfer steps are characterized by the standard rate constants $k_{s,1}$, $k_{s,2}$ and transfer coefficients $\alpha_1$, $\alpha_2$, while the regenerative steps are governed by the catalytic rate constants $k_{c,1}$ and $k_{c,2}$. Symbols S1 and S2 in sequences (b) and (d) stay for the side products, generated during the chemical regeneration steps, that do not participate in any of the electrode transformations.

### 2.2. *Mathematical description*

The mathematical description of the electrochemical system represented by sequences (a)–(d) in reaction scheme (I) is based on a series of partial differential equations; these represent the diffusion and chemical reaction as processes that govern the time and space-dependent concentrations of the redox species involved in electrode transformations (i.e., the initial reduced form R, the first oxidized intermediate Ox1, and the final oxidized product Ox2). In this mathematical model, it is assumed that the transport of all redox species occurs solely by semi-infinite linear diffusion toward

a stationary planar electrode, characterized by a uniform diffusion coefficient *D*. For each of the redox species involved in the electrode transformation, the rate of change in the corresponding concentration is described by a balance between the diffusive flux and the appropriate homogeneous chemical reaction term. The concentration of the reduced species R increases due to the regenerative EC′ reaction, in which Ox1 is converted back to R, and this contribution is included through the term $k_{c,1} \cdot c(\mathrm{Ox1})$. The intermediate redox species Ox1 is produced electrochemically at the surface of the electrode, consumed via the first regenerative chemical reaction (rate constant $k_{c,1}$), and regenerated again in the second step through the reaction of the final species Ox2, governed by the rate constant related to the second irreversible chemical step ($k_{c,2}$). The final species Ox2 is formed at the electrode in the second electron-transfer step, while it is depleted by the second homogeneous chemical reaction at the rate defined by the term $k_{c,2} \cdot c(\mathrm{Ox2})$. The differential equations in (1) to (3) reflect the dynamic interplay of diffusion and chemical reaction contributions that define the mathematical algorithm for the double-regenerative EC′EC″ mechanism.

$$\frac{\partial c(\mathrm{R})}{\partial t} = D \cdot \frac{\partial^2 c(\mathrm{R})}{\partial x^2} + k_{c,1} \cdot c(\mathrm{Ox1}) \quad (1)$$

$$\frac{\partial c(\mathrm{Ox1})}{\partial t} = D \cdot \frac{\partial^2 c(\mathrm{Ox1})}{\partial x^2} - k_{c,1} \cdot c(\mathrm{Ox1}) + k_{c,2} \cdot c(\mathrm{Ox2}) \quad (2)$$

$$\frac{\partial c(\mathrm{Ox2})}{\partial t} = D \cdot \frac{\partial^2 c(\mathrm{Ox2})}{\partial x^2} - k_{c,2} \cdot c(\mathrm{Ox2}) \quad (3)$$

### 2.3. *Boundary and initial conditions*

#### 2.3.1. *Boundary conditions at a distance (x) far away from the double layer i.e., for x → ∞*

The differential equations in (1) to (3) have been solved under the following boundary conditions:

– At large distances from the electrode surface (in the bulk of the solution, defined as $x \rightarrow \infty$), the concentrations of the reacting species remain unchanged by the electrochemical process. This is the classical semi-infinite diffusion assumption used for the mathematical modeling of electrochemical systems.

– The reduced form R exists in the bulk of the solution, and its initial concentration is not depleted far from the electrode during the electrochemical measurement. Its concentration in the bulk of the solution ($c(\mathrm{R})_{(\infty,\,t)}$) is therefore equal to its initial analytical concentration $c^*(\mathrm{R})$, i.e.,

$$c(\mathrm{R})_{(\infty,\,t)} = c^*(\mathrm{R}) \quad (4)$$

– The intermediate redox species Ox1 is formed only near the electrode during the first electron-transfer step, and its bulk concentration remains zero, i.e.,

$$c(\mathrm{Ox1})_{(\infty,\,t)} = 0 \quad (5)$$

– The final species of the electrode transformation Ox2 is also generated solely at or near the electrode, and does not exist in the bulk solution. Hence, its concentration in the bulk of the solution is:

$$c(\mathrm{Ox2})_{(\infty,\,t)} = 0 \quad (6)$$

#### 2.3.2. *Boundary conditions at time t > 0 at the electrode/electrolyte interface (x = 0)*

Relevant conditions for the theoretical model in (I) that hold at time $t > 0$ and a distance $x = 0$ (i.e., at the electrode/electrolyte interface) are described by Equations (7) to (9):

$$t > 0, \text{ and } x = 0;\ c(\mathrm{R}) + c(\mathrm{Ox1}) + c(\mathrm{Ox2}) = c^*(\mathrm{R}) \quad (7)$$

In addition, at $t > 0$, and $x = 0$, the flux of each electrochemically active species is directly related to the faradaic current associated with its electron-transfer reaction. According to Fick's first law,[1, 2, 6] the flux is proportional to the concentration gradient at the surface of the working electrode, and is defined by Equation (8):

$$D \cdot \frac{\partial c(\mathrm{R})}{\partial x} = -D \cdot \frac{\partial c(\mathrm{Ox1})}{\partial x} = \frac{I1(\mathrm{t})}{nFA} \quad (8)$$

The condition in (8) implies that the consumption/formation of redox species in the first electron transfer step at the working electrode/electrolyte interface is governed by the current of the first electron transfer step *I*1.

The equation that relates the interfacial flux of Ox1 to the faradaic current of the second electron-transfer step, in which Ox1 is further oxidized to Ox2, is defined by Equation (9):

$$D \cdot \frac{\partial c(\mathrm{Ox1})}{\partial x} = -D \cdot \frac{\partial c(\mathrm{Ox2})}{\partial x} = \frac{I2(\mathrm{t})}{nFA} \quad (9)$$

Together, the boundary conditions given in Equations (7)–(9) above link the interfacial electrochemical reactions with the mass transport of

redox-active species. This coupling ensures a physically meaningful solution to the differential equations in (1)–(3), which relate to both the diffusion and the homogeneous chemical reactions in the entire EC′EC″ mechanism.

Within the framework of the proposed mechanism, if kinetic constraints are assumed for both electron transfer steps, then corresponding forms of the Butler–Volmer relation at the electrode surface ($x = 0$, $t > 0$) can be applied to both electron transfer steps, as formulated in Equations (10) and (11):

$$\frac{I1}{n \cdot F \cdot A} = k_{s,1} \cdot e^{\alpha 1 \cdot \Phi 1} \cdot [c(\mathrm{R}) - e^{-\Phi 1} \cdot c(\mathrm{Ox1})] \quad (10)$$

$$\frac{I2}{n \cdot F \cdot A} = k_{s,2} \cdot e^{\alpha 2 \cdot \Phi 2} \cdot [c(\mathrm{Ox1}) - e^{-\Phi 2} \cdot c(\mathrm{Ox2})] \quad (11)$$

In Equations (10) and (11), symbols $\Phi 1$ and $\Phi 2$ represent dimensionless potentials, defined as $\Phi 1 = \frac{F}{RT}(E - E_1^{\ominus})$ and $\Phi 2 = \frac{F}{RT}(E - E_2^{\ominus})$, where $E_1^{\ominus}$ and $E_2^{\ominus}$ are the formal redox potentials of R/Ox1 and Ox1/Ox2 redox couples, respectively. In the definitions of $\Phi 1$and $\Phi 2$, $R$ is the symbol for the universal gas constant, $T$ is the thermodynamic temperature, $n$ is number of electrons exchanged ($n$ is set to one for both electron transfer steps), and $F$ is the Faraday constant. $A$ represents the effective area of the working electrode, while the parameters $\alpha 1$ and $\alpha 2$ in Equations (10) and (11) are the electron transfer coefficients for the first and second electron transfer steps, respectively. Within the framework of the considered EC′EC″ mechanism, the active surface of the working electrode can be formally regarded as a boundary at which two distinct faradaic processes take place. Accordingly, the first faradaic current ($I1$) can be formally attributed to the interfacial electron transfer between species R and Ox1, whereas the second ($I2$) corresponds to the interfacial electron transfer between Ox1 and Ox2. The homogeneous irreversible regenerative reactions Ox1 + Y → R and Ox2 + Y → Ox1 occur in the bulk solution, and their contributions are therefore incorporated into the diffusion–reaction differential equations (1) to (3). In contrast, the electrode kinetics are introduced exclusively through the interfacial boundary conditions expressed in Equations (10) and (11). The system of differential equations in (1)–(3) corresponding to the EC′EC″ mechanism was solved under the defined initial and boundary conditions by exploring the mathematical protocols described in.[6] A complete Mathcad working file developed for the calculation of square-wave voltammograms of the considered EC′EC″ mechanism is provided in the Supplementary Material of this study. A detailed description of the simulation protocols for an electrode mechanism in SWV, implemented in the Mathcad commercial platform, can be found in.[22]

### 2.4. *Definition of major parameters affecting the voltammmetric patterns*

Before starting an analysis of the theoretical results for the EC′EC″ mechanism, it is important to note that the analyzed effects will be interpreted primarily through the features of the forward and backward SWV current components. This approach enables a clearer insight into how variations in the governing kinetic parameters influence the voltammetric response. It is worth mentioning at this stage that the shapes and positions of the voltammetric profiles are affected by the square-wave amplitude ($E$sw), the potential step (d$E$), the temperature $T$ ($T$ = 298 K in all simulations), the number of electrons exchanged in each electron transfer step ($n$), and the electron-transfer coefficients $\alpha 1$ and $\alpha 2$ (both of which were set to 0.5 in all simulations).

In addition, the features of the voltammetric responses depend on four dimensionless kinetic parameters. The *dimensionless rate parameters for both electron transfer steps* ($K1$ and $K2$) are defined as $K1 = k_{s,2}/(Df)^{1/2}$ and $K2 = k_{s,2}/(Df)^{1/2}$. Both parameters ($K1$ and $K2$) combine the rates of electron transfer steps (via the standard rate constants of electron transfer $k_{s,1}$ and $k_{s,2}$) and those for mass transport (represented by the diffusion coefficient $D$, which was set to 0.000005 $cm^2s^{-1}$), relative to the time scale imposed by the square-wave frequency $f$. Furthermore, the chemical catalytic effects included in the EC′EC″ mechanism are described by two *dimensionless catalytic parameters* ($K$chem,1 and $K$chem,2), which are defined as follows: $K\mathrm{chem},1 = k_{c,1}/f$ and $K\mathrm{chem},2 = k_{c,2}/f$, where $k_{c,1} = k_{c,1}' \cdot c(\mathrm{Y})$ and $k_{c,2} = k_{c,2}' \cdot c(\mathrm{Y})$. In the latter equations, $k_{c,1}'$ and $k_{c,2}'$ are the intrinsic catalytic rate constants for the corresponding regenerative steps, while $c$(Y) is the molar concentration of the catalytic agent Y (assumed to be present in large excess in the voltammetric cell).

At this stage, it is important to emphasize that in biologically relevant enzymatic systems, the catalytic rate constants ($k_c'$) span several orders of magnitude, reflecting the diversity of biochemical turnover processes. Hence, slow catalytic steps associated with conformational rearrangements or

weak substrate interactions typically exhibit $k_c'$ values in the range $10^{-3}$–$10^{-1}$ $s^{-1}$,[5] whereas the majority of redox-active enzymes, including dehydrogenases, flavoproteins, and quinone-mediated systems, operate in an intermediate regime of approximately 0.1–$10^2$ $mol^{-3}$ L/s.[14] Highly efficient enzymes, such as peroxidases and components of respiratory electron-transfer chains, can reach much higher catalytic rates, on the order of $10^2$–$10^4$ $mol^{-3}$L/s,[5, 15] while diffusion-controlled biochemical reactions may have apparent rate constants of $10^6$–$10^8$ $mol^{-3}$L/s.[5] We note that the intermediate range of $k_c'$ values is the most relevant and experimentally accessible in voltammetric studies of EC′-type mechanisms,[1-6] where catalytic regeneration can be clearly resolved and quantitatively analyzed.

In the first series of analyses, a peak separation of 300 mV is imposed to allow for clear distinction of the features associated with each peak under different conditions. Although some of the simulated voltammograms correspond to conditions that may be difficult to realize experimentally, their analysis is valuable in terms of gaining deeper insight into the behavior of the entire EC′EC″ mechanism. The main objective of this theoretical analysis is to evaluate the catalytic effects by varying *K*chem,1 and *K*chem,2 and to discuss representative voltammetric patterns that facilitate a mechanistic interpretation and kinetic assessment of this complex electrode mechanism. During the simulations, all parameters are kept constant, except for a selected one that is varied to enable an unambiguous assessment of its specific effect on the voltammetric response. The complete Mathcad simulation file for the EC′EC″ mechanism is given in the Supplementary Material of this work.

## 3. RESULTS AND DISCUSSION

### 3.1. *Voltammetric patterns of the EC′EC″ mechanism simulated at a negligible rate for the first chemical regenerative reaction*

In the first series of simulated results (Fig. 1), the catalytic parameter of the first chemical regeneration step is kept negligible (i.e., *K*chem,1 = 0.0005), and the first peak associated with the R/Ox1 electrochemical conversion therefore remains largely unchanged across all of the conditions. Its forward and backward square-wave current components preserve the initial features over a large range of applied catalytic rates linked to the second electron transfer. This implies a scenario where no substantial homogeneous regeneration is coupled to the first electron-transfer step. In contrast, increasing the catalytic parameter of the second chemical regenerative step (with values of *K*chem, 2 varying in the range 0.0005–0.75, for example) produces a pronounced and systematic modification of the second peak. As *K*chem,2 increases, the second peak becomes progressively more intense, and gains a typical “catalytic-like” voltammetric signature. This is a consequence of enhanced chemical recycling involving feedback of the electroactive intermediate (Ox1), which is repeatedly oxidized in the second electron-transfer event. This enhancement is accompanied by a notable change in the balance between the forward and backward current components at the second peak, where the forward component becomes increasingly dominant and the backward component tends to become attenuated and reshaped. These features indicate that the system increasingly departs from a purely diffusion-controlled reversible response, and moves toward a chemical regeneration-controlled regime.[3,4,6] The resulting voltammetric pattern shows stronger peak amplification and a more persistent current contribution in the region of the second peak. Although a selective catalysis of only the second step is challenging from an experimental perspective (since the catalytic agent Y would normally influence both peaks), it provides a useful theoretical illustration, as it helps to isolate the behavior of the second regenerative loop and to clarify how the forward and backward components affect the increasing contribution of the catalytic chemical step in a controlled manner, while reducing the entire considered pathway to simpler EEC′ mechanistic scheme.[23] Under the circumstances considered here, the first peak has the features of a simple “E” mechanism,[1,6] while the second peak has attributes of an EC′ mechanism.[4-9] At this stage, it is worth emphasizing that in the SWV of an EC′ mechanism, the forward and backward current components differ from those observed in cyclic voltammetry because the current is sampled at the end of two successive potential pulses separated by a finite square-wave frequency. This time separation introduces a kinetic “memory” into the measurement, such that the electrochemical system does not fully relax between the forward and backward pulses, leading to a systematic separation of the two current components.[3] In contrast, under steady-state conditions in cyclic voltammetry involving catalytic EC′ mechanisms, the forward and backward currents often collapse into a single curve, since the system continuously adjusts to the applied potential and reaches a quasi-equilibrium at each point.[5] Conse-

quently, the intrinsic time discretization imposed by the square-wave frequency in SWV, coupled with the effect of the square-wave amplitude, always creates a measurable spacing between the forward and backward currents, whereas in cyclic voltammetry, these components may coincide when steady-state conditions are established. It should also be noted that when the rates of the regenerative chemical reactions in both electron-transfer steps are negligible, the overall mechanism is effectively reduced to a simple two-step sequential EE mechanism[24] (curve "**a**" in Fig. 1).

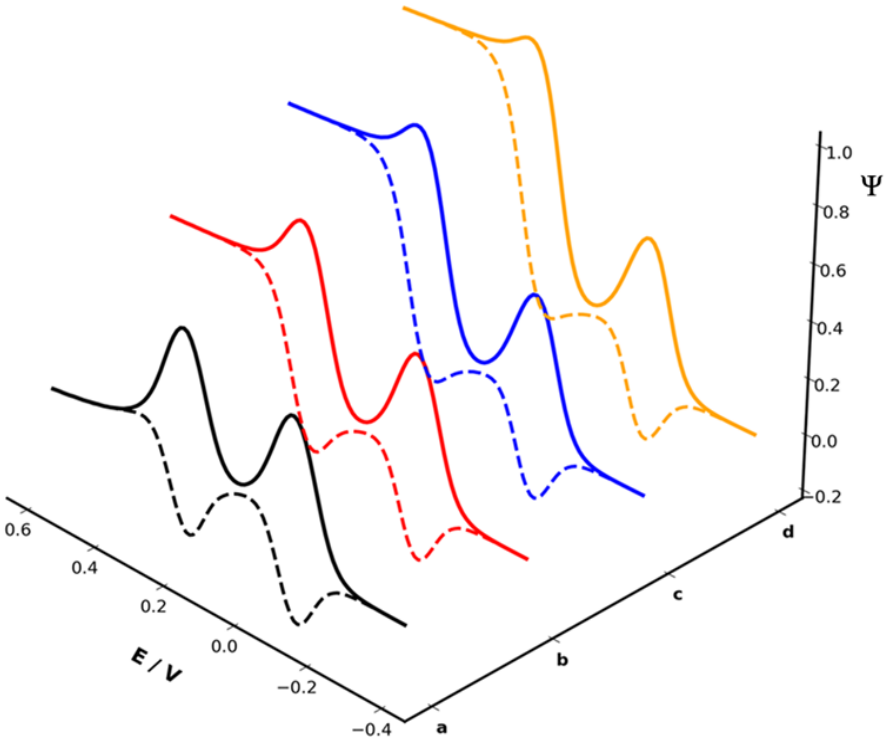


**Fig. 1**. Three dimensionless voltammetric patterns (forward and backward current components) of an EC′EC″ mechanism, simulated at a low rate of the first regenerative chemical step. For this series of voltammograms, the electron transfer coefficients were set to $\alpha 1 = \alpha 2 = 0.5$, while the dimensionless kinetic parameters of both electron transfer steps were set to $K1 = K2 = 5.623$. The dimensionless catalytic parameter for the first step was assumed to be negligible, and was set to $K\text{chem},1 = 0.0005$, while the dimensionless catalytic parameter of the second step $K\text{chem}, 2$ was set to values of: (a) 0.0005; (b) 0.1; (c) 0.5; (d) 0.75. The other conditions are a square-wave amplitude $E\text{sw} = 50$ mV, a potential step $dE = 10$ mV, temperature $T = 298.15$ K, and a potential separation between both peaks of 300 mV.

### 3.2. *Voltammetric patterns of the EC′EC″ mechanism simulated at a negligible rate for the second chemical regenerative reaction*

In the second scenario considered here, the catalytic regeneration is coupled primarily to the first electron-transfer step, as $K\text{chem},2$ is kept negligible (0.0005) while the value of $K\text{chem},1$ is increased from 0.0005 to 1 (Fig. 2). It is worth noting that this is a more realistic scenario than the selective catalysis of only the second step, since a catalytic agent often couples most strongly to the first-formed intermediate and can dominate the voltammetric response through the first regenerative loop.

As the magnitude of the dimensionless catalytic parameter related to the first electron transfer ($K\text{chem},1$) increases, the first peak becomes progressively more "catalytic-like" in its signature, followed by an increase in the overall current magnitude. This is because the chemical step rapidly converts the Ox1 species back to the initial redox active species, R, and continuously feeds the initial electroactive reactant during the time frame of the square-wave pulse. This chemical regeneration strengthens the forward component of the first peak and changes the balance between the forward and backward currents. The first peak also tends to broaden and to develop a more sustained current contribution around its potential region, a typical signature of EC′ behavior under square-wave conditions.[3,6]

In contrast, the second peak is much less affected across the series, since the catalytic pathway linked to the second electron-transfer step is essentially "switched off" by assigning a very small (negligible) value to *K*chem,2 in the model. The forward and backward components associated with the second interfacial conversion therefore retain a similar shape and relative separation, and any changes are mainly indirect, induced by the modified concentration profile of Ox1 created by the first catalytic loop. Under these conditions, the overall mechanism is effectively simplified to an EC′E scheme,[25] in which catalysis governs the first electron-transfer event while the second step behaves largely as a conventional electron-transfer process without significant regenerative feedback.

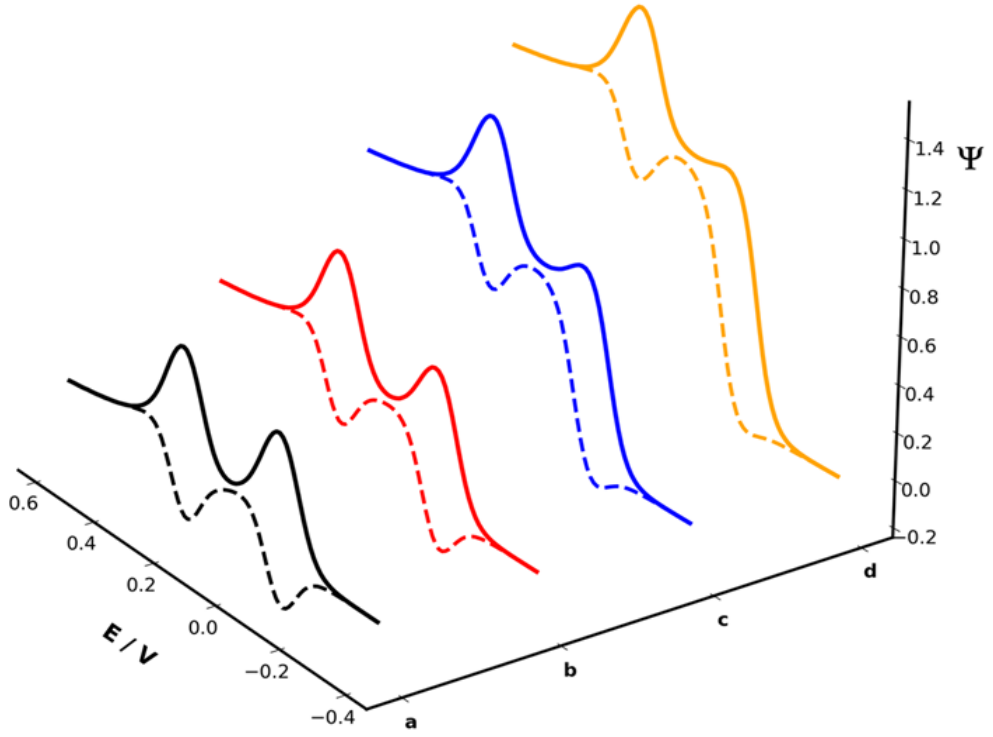


**Fig. 2**. 3D square-wave voltammetric patterns for the two-step double-regenerative EC′EC″ mechanism calculated at a negligible rate of the regenerative step related to the second electron transfer (*K*chem,2 = 0.0005). Voltammograms display the effect of the rate of the first regenerative step via the magnitude of Kchem,1 which was set to values of (a) 0.0005; (b) 0.1; (c) 0.5; (d) 1.0. The other simulation parameters were same as those in Figure 1.

### 3.3. *Voltammetry of the EC′EC″ mechanism at finite and equivalent rates of both chemical regenerative reactions*

In the scenario represented by the voltammetric curves in Figure 3, the regenerative substrate Y influences both electron-transfer steps equally, since the catalytic parameters *K*chem,1 and *K*chem,2 are set to identical values in the model. Under these conditions, both electron-transfer events exhibit clear EC′-type behavior, and each peak displays characteristic electrochemical-catalytic signatures. As the chemical regeneration becomes equally efficient for both steps, the forward current components of both peaks are enhanced, while the backward components are progressively suppressed. This results in identical amplification and reshaping of both voltammetric waves, characterized by sustained current contributions near the peak potentials and markedly enhanced currents in the post-peak region, due to the continuous resupply of electroactive material obtained via regenerative chemical reactions. The resulting response represents the full manifestation of the EC′EC″ mechanism, in which two coupled regenerative loops operate simultaneously and give rise to two catalytic waves. This scenario is particularly relevant from a mechanistic standpoint, as it illustrates how balanced catalytic coupling in both electron-transfer steps produces a symmetric catalytic response, and provides a clear framework for the analysis of complex multistep electrode processes under SWV conditions

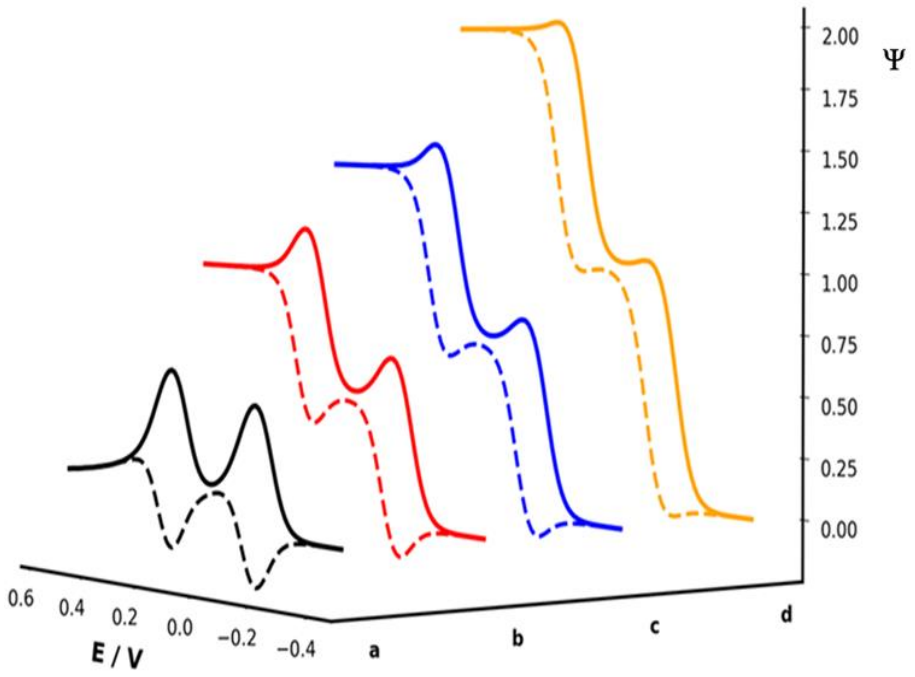


**Fig. 3.** 3D square-wave voltammetric patterns for the two-step double-regenerative EC′EC″ mechanism calculated at equal rates for both regenerative steps (*K*chem,1 = *K*chem,2), with values set to (a) 0.0005; (b) 0.25; (c) 0.5; (d) 1.0. The other simulation parameters were the same as those in Figure 1.

### 3.4. *Scenario with both electron transfer steps occurring at the same potential: Voltammetric patterns of the EC′EC″ mechanism at finite and equivalent rates for both catalytic reactions*

In the scenario considered in this part of the work, the two electron-transfer steps are positioned at essentially the same potential, so that their individual waves merge into a single composite voltammetric response (Figure 4). Although the underlying pathway is EC′EC″, the voltammetric patterns closely resemble those of a conventional one-step EC′ mechanism, since both electron transfer events and both regenerative loops are superimposed within the same potential window. As a consequence, the real mechanism becomes effectively "hidden" in the overall signal, and it is very difficult to determine from the voltammetric outputs alone whether the system follows a simple EC′ sequence or a two-step double-regenerative EC′EC″ pathway.

The influence of catalysis in Figure 4 is reflected by the systematic changes observed when *K*chem,1 and *K*chem,2 are increased simultaneously (for all curves in Figure 4, *K*chem,1 = *K*chem,2). At very low regenerative rates (curve "**a**" in Figure 4), the response is closer to a diffusion-controlled voltammetric peak with a pronounced backward component, indicating that regeneration is too slow for noticeable recycling of the electroactive species within the time scale of the square-wave (SW) pulses. When the catalytic parameters are increased to intermediate values (curve "**b**" in Figure 4), the peak becomes amplified and the forward component grows relative to the backward component, a finding that is consistent with the onset of efficient chemical recycling. At higher values of the catalytic rate parameters (curves "**c**", "**d**" and "**e**" in Figure 4), the response evolves toward a strongly catalytic regime, where regeneration is fast compared with the SW time scale, meaning that the current is sustained by rapid chemical resupply of electroactive material near the surface of the working electrode. In this limit, the backward component is increasingly suppressed and the overall response becomes dominated by the catalytic loop, the typical signature of EC′ behavior under square-wave excitation.[1, 3, 6]

From a kinetic viewpoint, these trends reflect a progressive shift from a regime in which electron transfer and diffusion define the response to a regime where homogeneous regeneration controls the local interfacial concentrations and sustains the current. Since both catalytic parameters are increased in parallel, the two regenerative cycles contribute in a concerted manner, and the system behaves as if there were a single effective regeneration pathway. From a thermodynamic view-

point, the coincidence of the two formal potentials removes the most obvious diagnostic feature, namely peak separation, and the merged wave therefore carries limited information on the presence of two distinct electron-transfer steps. Unless additional constraints are introduced to the theoretical model, the observable response under such conditions is expected to be indistinguishable from that of a single-step EC′ mechanism.

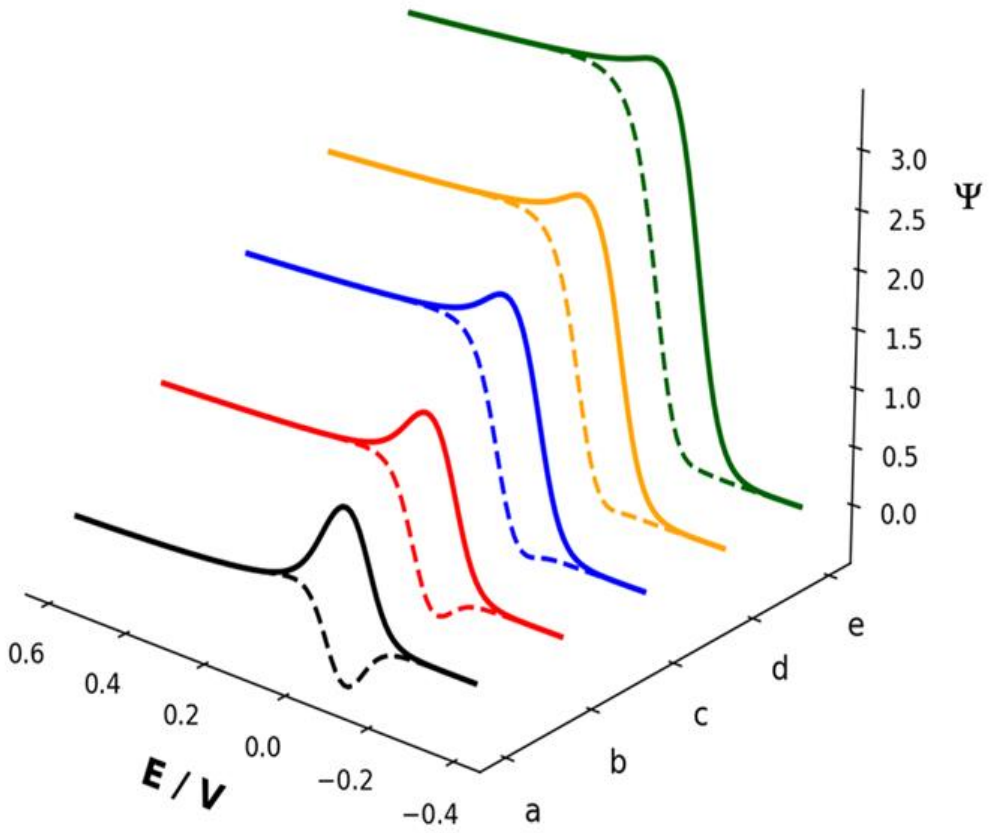


**Fig. 4**. 3D voltammetric curves for the two-step double-regenerative EC′EC″ mechanism, simulated under the assumption that both electron transfer steps occur at same potential. Curves are calculated at equal rates of both regenerative steps (*K*chem,1 = *K*chem,2), with values of (a) 0.001; (b) 0.25; (c) 2.5; (d) 5; (e) 10. The other simulation parameters were same as those used in Figure 1.

### *3.5. Scenario with both electron transfer steps separated by 150 mV at the potential scale: Voltammetric patterns of the EC′EC″ mechanism for a negligible rate of the second catalytic reaction*

In this set of simulations, the catalytic regeneration is effectively confined to the first electron-transfer step, since *K*chem,2 is kept negligible (0.001) while *K*chem,1 is increased over several orders of magnitude. At a small value of *K*chem,1 (curve "**a**" in Figure 5), the response still shows two discernible waves separated by 150 mV, and the second peak retains a relatively normal appearance since it is not affected by a regenerative loop. As *K*chem,1 is increased to moderate values (curves "**b**" and "**c**" in Figure 5), the first peak becomes progressively amplified and reshaped, reflecting the increasingly efficient chemical recycling of the product of the first electron-transfer step back to the electroactive reactant within the square-wave time scale. In parallel, the forward component of the first peak becomes more dominant, while the backward component is suppressed and distorted, an effect that is consistent with the onset of EC′-type behavior.

When *K*chem,1 reaches high values (curves "**d**" and "**e**" in Figure 5), the first catalytic wave becomes so intense and broad that its potential-domain "footprint" extends into the region where the second electron-transfer step would normally produce a separate peak. Under these conditions, the second peak becomes engulfed and effectively merged into the tail and plateau-like region of the first catalytic response. This occurs because the rapid regeneration maintains a high near-surface concentration of the electroactive species associat-

ed with the first step, while sustaining the current over a wider potential interval and masking the more limited contribution of the second step (which is assumed to remain essentially "non-catalytic"). The net effect is a composite waveform in which the mechanistic signature of the second electron transfer is strongly attenuated and can no longer be resolved as a distinct feature, despite the nominal 150 mV separation between the formal potentials of both electron transfer steps.

From a mechanistic standpoint, this behavior indicates that the system is approaching the EC′EC limit,[25] where the first step dominates the overall response and it becomes difficult to diagnose the second step from the voltammogram, especially at high rates for the regenerative step. At a sufficiently large value of *K*chem,1, distinguishing this EC′E limit from a simple one-step EC′ mechanism becomes challenging under the given conditions, because the dominant catalytic wave can obscure the presence of the second electron-transfer event. In practice, reliable discrimination would then require additional instrumental alterations, such as changing the SW signal parameters (potential step or SW amplitude).

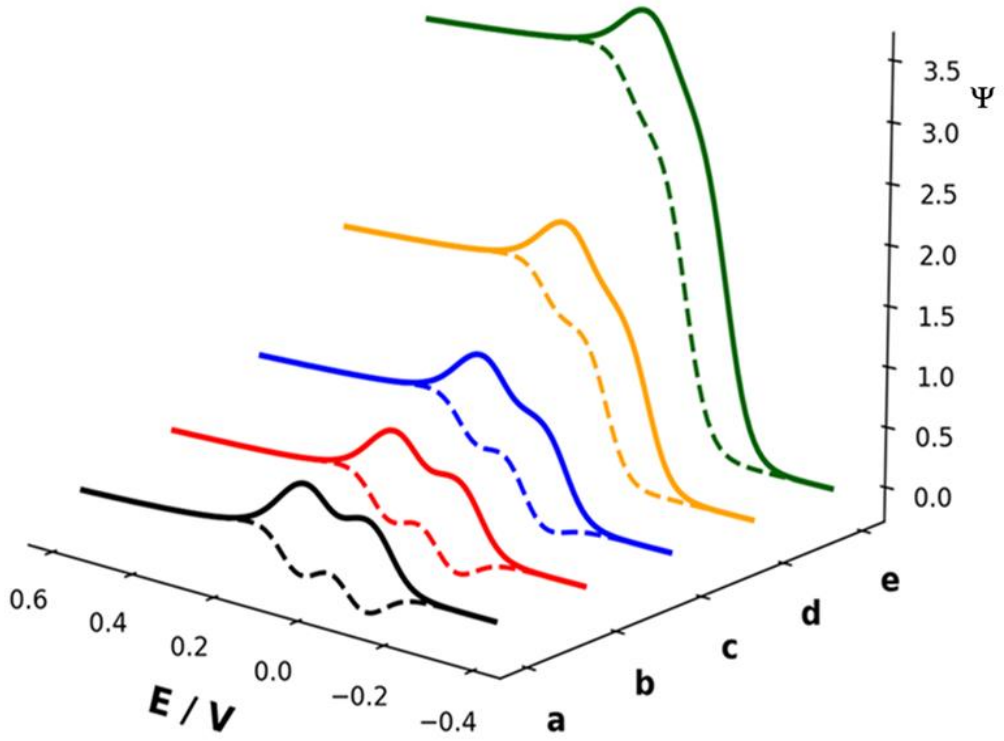


**Fig. 5**. 3D voltammetric curves of the two-step double-regenerative EC′EC″ mechanism, simulated under the assumption that both electron transfer steps differ by 150 mV at the potential scale. Curves are calculated at a negligible rate for the second regenerative step (*K*chem,2 = 0.001), while the rate of the first regenerative step *K*chem,1 is set to values of (a) 0.001; (b) 0.25; (c) 0.5; (d) 2.5; and (e) 10. The other simulation parameters were identical to those used in Figure 1.

## 4. CONCLUSIONS

In this work, the two-step double-regenerative EC′EC″ mechanism has been treated theoretically for the first time under the kinetic regime in SWV. The model presented here provides a comprehensive and unified framework for analyzing multistep electron-transfer processes coupled with dual regenerative chemical reactions. An analysis of the theoretical results shows that SWV is particularly sensitive to the interplay between electron-transfer kinetics, homogeneous regeneration, and diffusional mass transport, allowing the relevant mechanistic features to be defined through an analysis of the forward and backward current components. One of the major benefits of a theoretical consideration of the EC′EC″ framework is its ability to capture, within a single mathematical algorithm, a broad spectrum of mechanistic behaviors that emerge as limiting cases when specific kinetic parameters are varied in a defined manner. Hence, from a mechanistic point of view, the EC′EC″

electrochemical scheme encompasses important limiting scenarios, including the E, EE, EC′E, EEC′ mechanisms, and also a single-step EC′ mechanism. This versatility makes the EC′EC″ pathway a powerful theoretical platform for gaining insight into how regenerative processes affect the voltammetric responses without the need to reformulate the mathematical algorithm. By tuning the relative magnitudes of the catalytic parameters and electron-transfer rates in the model, smooth transitions between different mechanistic regimes can be achieved.

The relevance of this mechanism extends beyond theoretical electrochemistry, as many physiological and biochemical systems rely on sequential two-step electron transfer pathways that are coupled to regenerative reactions by enzymes, cofactors, or various redox mediators. The EC′EC″ framework therefore provides a useful theoretical playground for understanding redox processes in living organisms, such as metabolic electron-transfer chains and redox cycling phenomena, in which intermediate species are continuously regenerated and reused. The ability to describe such mechanisms within a single electrochemical model opens up new opportunities for interpreting the redox behavior of complex biochemical systems, and for extracting relevant kinetic information from experimental data. For experimentalists, the extensive set of simulated voltammograms presented in this work offers practical guidance on how different kinetic and thermodynamic parameters manifest in square-wave voltammetric outputs. The results elaborated in this work illustrate which voltammetric features are diagnostic, which are masked under certain conditions, and where mechanistic ambiguity is unavoidable. In particular, the simulations highlight conditions under which complex two-step double-regenerative behavior may be indistinguishable from simpler mechanisms, with emphasis on the need for careful experimental design and parameter variation when interpreting SWV data.

At the same time, the limitations of the EC′EC″ model should be also acknowledged. The mechanism is based on the assumption of well-defined sequential electron-transfer steps and homogeneous regeneration reactions, and does not explicitly account for complications such as adsorption, surface-confined intermediates, or other coupled chemical reactions. Nevertheless, within its intended scope, the EC′EC″ mechanism represents one of the very few theoretical frameworks[38] that explicitly link two electron-transfer steps with two regenerative chemical processes in a consistent manner. As such, it provides a valuable framework for future theoretical developments, and can be seen as a valuable reference point for experimental studies of complex regenerative multi-step redox systems.

Finally, it should be emphasized that frequency analysis alone in SWV is not sufficient for extracting mechanistic or kinetic information for the EC′EC″, as the frequency simultaneously affects several of the kinetic parameters involved in this complex mechanism.[6,26-33] Consequently, the use of frequency as a primary diagnostic variable is not reliable in this case under SW voltammetric conditions, and alternative experimental strategies[34-37] are recommended for consistent mechanistic and kinetic interpretations. To obtain access to the relevant kinetic parameters for all of the elementary steps in the EC′EC″ mechanism, one may take advantage of the experimental protocols proposed in [3], as these are particularly applicable in situations where the two electron-transfer steps are well separated, typically by at least 200 mV on the potential scale. In addition, in the case of multistep catalytic mechanisms, access to the standard rate constants of both electron-transfer steps, as well as to the corresponding electron-transfer coefficients, can be achieved by exploiting advanced kinetic analysis methods. In particular, the amplitude-based quasi-reversible maximum approach,[35] step potential analysis,[36] and methodologies involving electrochemical faradaic spectroscopy[34] provide powerful and complementary routes for extracting these kinetic parameters under conditions where conventional techniques are insufficient.

**Acknowledgments:** The author is grateful to the Goce Delčev University, Štip, for permanent support, and to the Alexander von Humboldt Foundation (Germany) for support via research group linkage project with Ref 3.4 - 1070534 - MKD - IP.

## REFERENCES

(1) Compton, R. G.; Banks, C. E. *Understanding Voltammetry*, 2nd ed.; Imperial College Press, London, **2011**.

(2) Bard, A. J.; Faulkner, L. R. *Electrochemical Methods, Fundamental and Applications*; Wiley, New York, **2001**.

(3) Gulaboski, R.; Mirceski, V. New aspects of the electrochemical-catalytic (EC′) mechanism in square-wave voltammetry. *Electrochim. Acta* **2015**, *167*, 219–225. https://doi.org/10.1016/j.electacta.2015.03.175

(4) Gulaboski, R.; Petkovska, S. A time-independent approach to evaluate the kinetics of enzyme-substrate reactions in cyclic staircase voltammetry. *Anal. Bioanal. Electrochem.* **2018**, *10*, 566–575.

(5) Saveant, J. M.; Costentin, C. *Elements of Molecular and Biomolecular Electrochemistry: An Electrochemical Approach to Electron-Transfer Chemistry*, 2nd ed.; Wiley, Hoboken, NJ, **2019**. DOI:10.1002/9781119292364

(6) Mirceski, V.; Komorsky-Lovric, S.; Lovric, M. *Square-Wave Voltammetry: Theory and Application* (Scholz, F. Ed.) Springer, Berlin, **2007**.

(7) O'Dea J. J.; Osteryoung, J.; Osteryoung, R. A. Theory of square-wave voltammetry for kinetic systems. *Anal. Chem.* **1981**, *53*, 4, 695–701. https://doi.org/10.1021/ac00227a028

(8) Osteryoung, J. A.; Osteryoung, R. Square-wave voltammetry. *Anal. Chem.* **1985**, *57*, 101–110. https://doi.org/10.1021/ac00279a004

(9) Deamer, D. Electrochemical energy for living systems. *Curr. Opin. Electrochem.* **2021**, *29*, 100742. DOI: 10.1016/j.coelec.2021.100742

(10) Fourmond, V.; Wiedner, E. S.; Shaw, W. J.; Leger, C. Understanding and design of bidirectional and reversible catalysts of multi-electron, multistep reactions. *J. Am. Chem. Soc.* **2019**, *141*, 11269–11285. https://doi.org/10.1021/jacs.9b04854

(11) Hagras, M. A.; Stuchebrukhov, A. A. Concerted two-electron reduction of ubiquinone in respiratory Complex I. *J. Phys. Chem. B* **2019**, *123*, 5265–5273. https://doi.org/10.1021/acs.jpcc.9b07536

(12) Haapanen, O.; Sharma, V. Redox and protonation state driven substrate-protein dynamics in respiratory Complex I. *Curr. Opin. Electrochem.* **2021**, *29*, 100741. https://doi.org/10.1016/j.coelec.2021.100741

(13) Lopez-Tenes, M.; Gonzalez, J.; Molina, A. Two-electron transfer reactions in electrochemistry for solution-soluble and surface-confined molecules: A common approach. *J. Phys. Chem. C* **2014**, *118*, 12312–12324. DOI: 10.1021/jp5025763

(14) Sies, H.; Parker, L. Quinones and quinone enzymes. In: *Methods in Enzymology*; Academic Press, London, U.K., **2004**.

(15) Nolfi-Donegan, D.; Braganza, A.; Shiva, S. Mitochondrial electron transport chain: Oxidative phosphorylation, oxidant production, and methods of measurements. *Redox Biol.* **2020**, *37*, 101674. https://doi.org/10.1016/j.redox.2020.101717

(16) Parey, K.; Wirth, C.; Vonck, J.; Zickermann, V. Respiratory Complex I – Structure, mechanism and evolution. *Curr. Opin. Struct. Biol.* **2020**, *63*, 1–9. DOI: 10.1016/j.sbi.2020.01.004

(17) Gulaboski, R.; Markovski, V.; Zhu, J. Redox chemistry of coenzyme Q-A short overview of the voltammetric features. *J. Solid State Electrochem.* **2016**, *20*, 3229–3238. https://doi.org/10.1007/s10008-016-3230-7

(18) Quan, M.; Sanchez, D.; Wasylkiw, M. F.; Smith, D. K. Voltammetry of quinones in unbuffered aqueous solution: Reassessing the roles of proton transfer and hydrogen bonding in the aqueous electrochemistry of quinones. *J. Am. Chem. Soc.* **2007**, *129*, 12847–12856. https://doi.org/10.1021/ja0743083

(19) Bogeski, I.; Gulaboski, R.; Kappl, R.; Mirceski, V.; Stefova, M.; Petreska, J.; Hoth, M. Calcium binding and transport by coenzyme Q. *J. Am. Chem. Soc.* **2011**, *133*, 9293–9303. doi.org/10.1021/ja110190t

(20) Batchelor-McAuley, C.; Compton, R.G. Voltammetry of multi-electron electrode processes of organic species. *J. Electroanal. Chem.* **2012**, *669*, 73–81. https://doi.org/10.1016/j.jelechem.2012.01.016

(21) Warren, J. J.; Tronic, A. T.; Mayer, J. M. Thermochemistry of proton-coupled electron transfer reagents and its implications. *Chem. Rev.* **2010**, *110*, 6961–7001. https://doi.org/10.1021/cr100085k

(22) Gulaboski, R.; Mirceski, V. Calculating of square-wave voltammograms-A practical on-line simulation platform. *J. Solid State Electrochem.* **2024**, *28*, 1121–1130. https://doi.org/10.1007/s10008-023-05520-y

(23) Kokoskarova, P.; Lazarova, S.; Papakoca, K.; Gulaboski, R. Theoretical analysis of two-step EEC′ mechanism in Square-wave voltammetry: Application to water soluble redox systems with inverted potentials. *Anal. Bioanal. Electrochem.* **2025**, *17*, 476–496. 10.22034/abec.2025.725967

(24) Gulaboski, R.; Mirceski, V. Square-wave voltammetry of two-step diffusional electrode mechanism coupled with a reversible follow-up chemical reaction. *J. Solid State Electrochem.* **2021**, *25*, 2893–2901. https://doi.org/10.1007/s10008-021-05027-4

(25) Laborda, E.; Gonzalez, J.; Molina, A. Nuances of the voltammetry of homogeneous multi-electron molecular catalysts: An analytical theory for two-electron catalysis. *J. Catal.* **2022**, *407*, 232–240. https://doi.org/10.1016/j.jcat.2022.01.014

(26) Gulaboski, R. The future of voltammetry, *Maced. J. Chem. Chem. Eng.* **2022**, *41*, 151–162. https://doi.org/10.20450/mjcce.2022.2555

(27) Gulaboski, R.; Mirčeski, V.; Lovrić, M. Critical aspects in exploring time analysis for the estimation of kinetic parameters of surface electrode mechanisms coupled with chemical reactions. *Maced. J. Chem. Chem. Eng.* **2021**, *40*, 1–9. https://doi.org/10.20450/mjcce.2020.2152

(28) Costentin C.; Saveant, J.-M. Multielectron molecular catalysts of electrochemical reactions: Benchmarking of homogeneous catalysts. *ChemElectroChem* **2014**, *1*, 1226–1236. https://doi.org/10.1002/celc.201300263

(29) Sylvia, S. V.; Rajendran, L. Cyclic voltammetric response of homogeneous catalysis of electrochemical reactions: Part 2. A theoretical and numerical approach for EC scheme. *J Electroanal. Chem.* **2022**, *918*, 116453. https://doi.org/10.1016/j.jelechem.2022.116453

(30) Rasi, M.; Rajendran, L.; Subbiah, A. Analytical expression of transient current-potential for redox enzymatic homogeneous system. *Sens. Actuators, B. Chem.* **2015**, *208*, 128–136. https://doi.org/10.1016/j.snb.2014.11.006

(31) Molina, A.; Gonzalez, J.; Laborda, E.; Wang, Y.; Compton, R.G. Analytical theory of the catalytic mechanism in square-wave voltammetry at disc electrodes. *Phys. Chem. Chem. Phys.* **2011**, *37*, 16748–16755. https://doi.org/10.1039/C1CP22032B

(32) Nicholson, R. S. Theory and application of cyclic voltammetry for measurement of electrode reaction kinetics. *Anal. Chem.* **1965**, *37*, 1351–1355. DOI: 10.1021/ac60230a016

(33) Andrieux, C. P.; Blocman, C.; Dumas-Bouchiat, J. M.; M'Halla, F.; Saveant, J. M. Homogeneous redox catalysis of electrochemical reactions: Part V. Cyclic voltammetry. *J. Electroanal. Chem.* **1980**, *113*, 19–40. https://doi.org/10.1016/S0022-0728(80)80508-0

(34) Jadreško, D.; Guziejewski, D.; Mirčeski, V. Electrochemical faradaic spectroscopy. *ChemElectroChem.* **2018**, *5*, 187–194. https://doi.org/10.1002/celc.201700784

(35) Mirceski, V.; Laborda, E.; Guziejewski, D.; Compton, R. G. New approach to electrode kinetic measurements in square-wave voltammetry: Amplitude-based quasi-reversible maximum. *Anal. Chem.* **2013**, *85*, 5586–5594. https://doi.org/10.1021/ac4008573

(36) Mirceski, V.; Stojanov, L.; Ogorevc, B. Step potential as a diagnostic tool in square-wave voltammetry of quasi-reversible electrochemical processes. *Electrochim. Acta* **2019**, *327*, 134997. https://doi.org/10.1016/j.electacta.2019.134997

(37) Gulaboski, R.; Mirceski, V. Application of voltammetry in biomedicine-Recent achievements in enzymatic voltammetry. *Maced. J. Chem. Chem. Eng*. **2020**, *39*, 153–166. https://doi.org/10.20450/mjcce.2020.2152

(38) Lopes-Tenes, M.; Laborda, E.; Martinez-Ortiz, F.; Gonzalez, J.; Molina A. Square-wave voltammetry as a powerful tool for studying multi-electron molecular catalyst. *J. Electroanal. Chem.* **2022**, *927*, 116943. https://doi.org/10/1016/j/jelechem.2022.116943